III International Conference on Particle-based Methods – Fundamentals and Applications
PARTICLES 2013
M. Bischoff, E. Oñate, D.R.J. Owen, E. Ramm & P. Wriggers (Eds)

# FLOW CONDITIONING MODELING AND APPLICATION TO PARTICLE METHOD

**CEZAR AUGUSTO BELLEZI[1]*, FABIO KENJI MOTEZUKI[2], LIANG-YEE CHENG[2] AND KAZUO NISHIMOTO[1]**

[1]Department of Naval and Ocean Engineering
Escola Politécnica of University of São Paulo
Av. Prof. Mello Moraes, 2231, São Paulo – SP, Brasil
e-mail: polinaval@usp.br, web page : http://www.pnv.poli.usp.br

[2] Department of Construction Engineering
Escola Politécnica of University of São Paulo
Av. Prof. Almeida Prado, 83, São Paulo – SP, Brasil
web page: http://www.pcc.usp.br

*cbellezi@tpn.usp.br

**Keywords:** Moving Particle Simulation, MPS, boundary condition, vortex sheet.

**Abstract.** This work comprises the development of a re-circulation boundary condition to simulate the flow around a cylinder using the Moving Particles Simulation (MPS). The re-circulation boundary condition consists in the re-injection of the fluid particles that flows out the downstream boundary of the computational domain into the upstream boundary through the application of a periodic boundary condition, and a flow conditioner that comprises a region where the velocities of the fluid particles are gradually adjusted to a uniform flow by suppressing the velocity perturbations. The proposed recirculation boundary condition is applied to simulate the flow around a fixed cylinder and the vortex sheet formation process. The *Strouhal Number* x *Reynolds Number* diagram obtained using the MPS method show results close to those present in literature. For the laminar flow, the streamlines of MPS simulations show similarity with experimental results present in literature.

## 1 INTRODUCTION

A large number of fluid flow applications for the offshore industry are modeled as external unidirectional flow phenomena. The vortex induced vibration on slender structures, such as pipelines, risers and columns of semisubmersible platforms, and the hydrodynamic forces over a hull, due to wave, seas current or vessel progression, are important examples of this modeling.

In the present study the Moving Particle Simulation (MPS) method is used for the simulation of these phenomena, developed by [1]. The MPS is a fully lagrangian meshless method for incompressible flow, in which the differential operators are derived from a particle interaction model based on weight average of the contribution of the neighborhood particle. The advantages of applying the lagrangian particle-based method in the simulation of the

predominantly unidirectional flow phenomena are related to the flexibility and easy modeling of fluid-structure interaction with complex geometries and multi-body dynamics. Some of the examples of the applications of the MPS method in complex fluid-structure interaction can be found in the studies carried by the authors [2], [3] among others.

A challenge in the simulation of predominantly unidirectional flow phenomena using particle methods is the modeling of outflow boundary conditions. The most common approach used on outlet boundaries consists in the removal of the particles that passes through the outlet boundary, i.e., downstream boundary of the computational domain. The present study proposes an alternative solution, consisting in a recirculation boundary condition that operates in a way similar to a shortened recirculation tunnel or canal, and it is composed by a periodic boundary condition, which connects the inlet and outlet boundaries, combined with a flow conditioner.

In the recirculation boundary condition, when the particles downstream of the body, reaches the outlet boundary, they are re-injected to the upstream of the inlet boundary, i.e., the upstream boundary of the computational domain, by applying a periodic boundary condition. After the re-injection, the particles pass through a flow conditioning region where the particle motions are adjusted gradually to the values expected at the inlet of the effective computational domain. The flow conditioning is based on an artificial damping of the difference between the particle velocity and the desired upstream flow velocity, and is carried out at the explicit step of the MPS method. This solution provides a simpler setting of pressure and particle number density boundary conditions at inlet and outlet boundaries, with more stable computation, and enables a simpler computation, with no need of dynamic memory allocation due to new particles creation and old particles removal.

This study comprises the formulation of the recirculation, by given the detailed description of the periodic boundary condition and the flow conditioner, and shows a simple example of application. The application consists in the two-dimensional simulation of the flow around a cylinder for different Reynolds numbers and its comparison to experimental results present in the literature. The Reynolds Number x Strouhal Number diagram obtained using MPS method is compared to results in literature. In addition, the configuration of the streamlines using the particle simulation, for laminar flow Reynolds range, is compared to results in available literature.

## 2 MOVING PARTICLE SEMI-IMPLICT METHOD

This section contains a brief description of the MPS method. The governing equations of the incompressible flow are the mass conservation equation (Eq. 1) and the momentum conservation equation (Eq. 2)

$$\frac{D\rho}{Dt} = -\rho(\nabla.\vec{u}) = 0 \tag{1}$$

$$\frac{D\vec{u}}{Dt} = -\frac{1}{\rho}\nabla \mathrm{P} + \vartheta\nabla^2\vec{u} + \frac{\vec{f}}{\rho} + \vec{g} \tag{2}$$

where $\rho$ is the fluid density, $u$ the fluid velocity, $P$ the pressure, $g$ the gravitational acceleration, $f$ the external forces, $\vartheta$ the kinematic viscosity and $t$ the time.

In MPS method, the differential operators are replaced by operators derived from a particle-interaction model based on the weighting contribution of each particle inside a

neighborhood radius. The particle weight function is (Eq. 3)

$$\omega(r) = \begin{cases} \frac{r_e}{r} - 1 \; for \; (0 \leq r < r_e) \\ 0 \; for \; (r_e \leq r) \end{cases} , \tag{3}$$

where $r = \left|\vec{r_j} - \vec{r_i}\right|$ is the distance between two particles $i$ and $j$ and $r_e$ is the neighborhood radius. The particle number density (*pnd*) (Eq. 4) is proportional to the fluid density and this parameter is used to impose the incompressibility.

$$[pnd]_i = \sum_{j \neq i} \omega(|\vec{r_j} - \vec{r_i}|) \tag{4}$$

The gradient operator and the laplacian operator of a scalar function $\Phi$ are given by Eq. 5 and Eq. 6, respectively:

$$[\nabla \Phi]_i = \frac{d}{pnd^0} \sum_{j \neq i} \left[ \frac{(\Phi_j - \Phi_i)}{|\vec{r_j} - \vec{r_i}|^2} (\vec{r_j} - \vec{r_i}) \omega(|\vec{r_j} - \vec{r_i}|) \right] \tag{5}$$

$$[\nabla^2 \Phi]_i = \frac{2d}{pnd^0 \delta} \sum_{j \neq i} \left[ (\Phi_j - \Phi_i) \omega(|\vec{r_j} - \vec{r_i}|) \right] , \tag{6}$$

where $d$ is the number of dimension and $pnd^0$ is the initial particle distance number value, and the $\delta$ constant is given by Eq. 7.

$$\delta = \frac{\int_V \omega(r) r^2 dv}{\int_V \omega(r) dv} \tag{7}$$

MPS method adopts a semi-implicit algorithm, which is divided in two parts. The first part consists on the explicit calculation of velocity, position and *pnd* of the particles considering the terms on the right side of the Navier-Stokes equation (Eq. 2), except the pressure gradient. The seconds part is composed by the implicit calculation of the pressure, solving a linear system of Poisson equation (Eq. 8) derived from mass conservation for incompressible flow.

$$[\nabla^2 P^{n+1}]_i = -\frac{\rho}{\Delta t^2} \frac{[pnd^*]_i - pnd^0}{pnd^0} \tag{8}$$

where *pnd** is the *pnd* value estimated at the explicit part.
Finally, by using the pressure calculated implicitly, the correction of the velocity estimated at the explicit part is carried out by accounting the pressure gradient term.

The rigid wall is modeled according to [1] as three layers of particles. The first layer is composed by the particle that may be in contact with the fluid. These particles are considered during the calculation of pressure. The adjacent two layers are composed by dummy particles, which are employed to assure the correct calculation of the *pnd* parameter at wall particles of the first layer. The motion of the wall particles is imposed as input parameter at the explicit step of the algorithm.

The flowchart showing the MPS algorithm is presented at the Figure 1. The simulations carried out in the present study are performed by using the MPS code of the Numerical Offshore Tank Laboratory of the University of São Paulo.

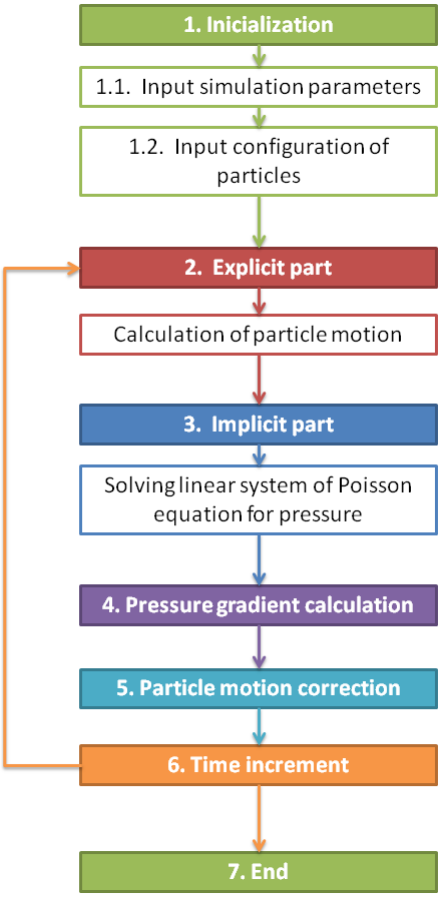


**Figure 1** MPS algorithm flowchart

## 3 RE-CIRCULATION TECHNIQUE

Focusing on the investigation of the flow around arbitrary shaped moving bodies, the numerical technique proposed herein consists essentially the modelling of a recirculation boundary condition, which is composed by the development of a periodic boundary condition and a flow conditioning technique for the particle-based simulation.

The paradigm used in the explanation of the re-circulation and flow conditioning technique is presented in the Figure 2. For sake of simplicity, the example of two-dimensional flow around a circular cylinder is considered. In the top of Figure 2, it is presented the traditional technique based on inflow and outflow boundaries, which injects new particles at the upstream boundary and eliminates the particles that reach the downstream boundary of the computational domain. In the bottom of Figure 2, it is presented the recirculation boundary condition proposed herein, in which the particles that flow out the downstream boundary of the computational domain are re-injected into its the extended upstream boundary of the computational domain, and from the upstream boundary, the velocities of the fluid particles is gradually adjusted when they passes through the flow conditioning region.

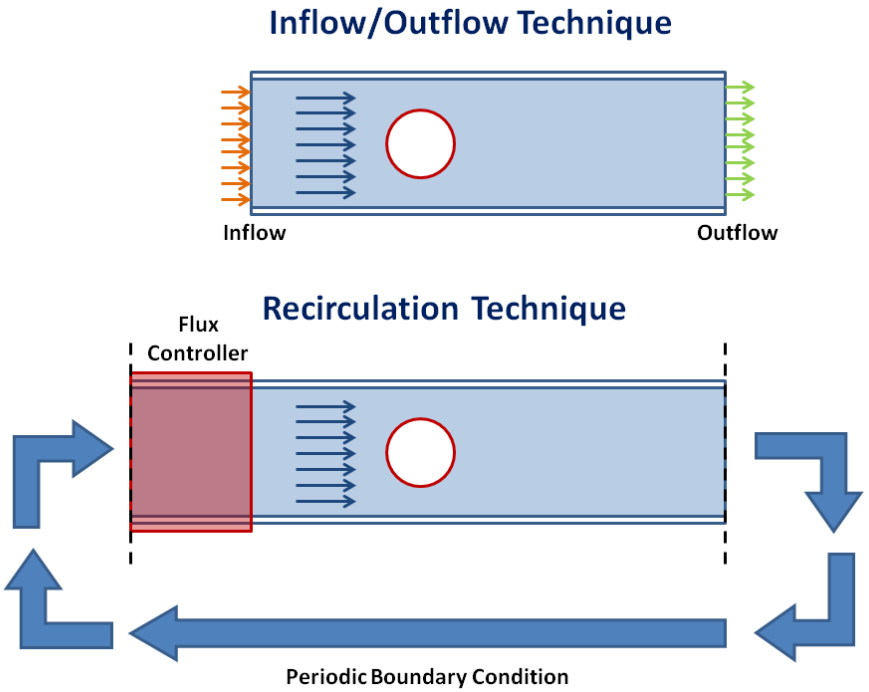


**Figure 2** Inflow/outflow boundaries *x* Recirculation technique

### 3.1 Periodic boundary condition

Periodic boundary conditions are applied in cases where a phenomenon repeats cyclically in space. In the periodic boundaries, illustrated as a dashed lines in Figure 3, when a particle flows out of the computational domain it is reintroduced with the same physical properties in the opposite side of the domain as illustrated in Figure 3-a. In the case of the flow around a cylinder, the fluid particles that reach the downstream boundary are re-injected into the upstream boundary of the computational domain.

When calculating the differential operators of the particles near the periodic boundary condition, the particles in the opposite side also have to be considered. As an example, Figure 3-b shows the red particles that should be considered in the calculation of the gradient operator of the green particle, despite they are in the opposite side of the computational domain. The gray particles are the positions where the red particles should be for the calculation. In this way, the red particles are numerically displaced by the distance of the computational domain when the differential operator at the position of the green particle is evaluated. This procedure simplifies the code implementation for the assessment of the differential operators and the solution of the linear equation system considering the periodic boundary condition.

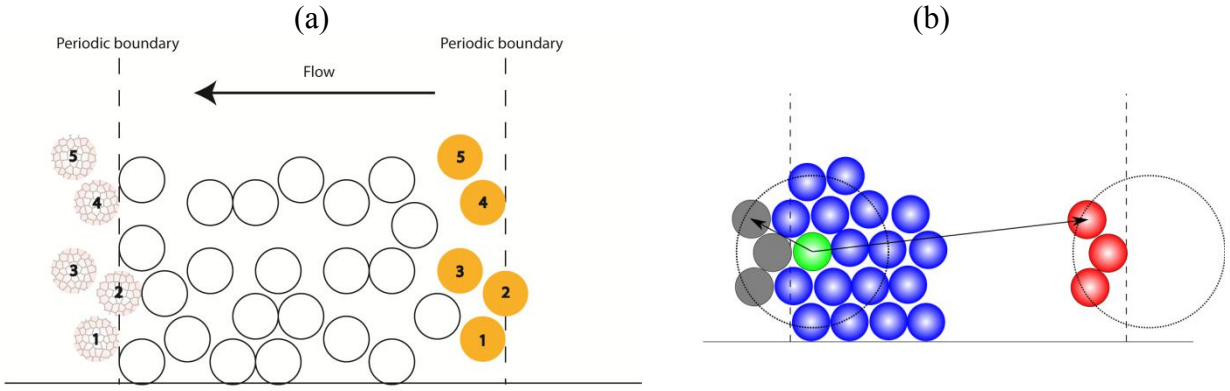


**Figure 3** Periodic boundary condition

### 3.2 Flow conditioner

In the modeling of the flow around a body, if only the periodic boundary condition is applied, the velocity perturbations downstream the body will be introduced in the flow upstream the body. In order to provide and maintain the desired flow profile, generally to reproduce the far field flow without perturbation, a flow conditioning technique is proposed.

The main functions of the flow conditioner are: to suppress mean or fluctuating variations in transverse velocity; and to adjust the velocity on the flow direction, which resemble, respectively, the honeycomb inside the setting chamber and propellers of a wind tunnel, but gathered together. The flow conditioner used in the simulation of the flow around a cylinder is presented in Figure 4. Here, x axis is defined as the flow direction and y axis the transverse to the flow direction.

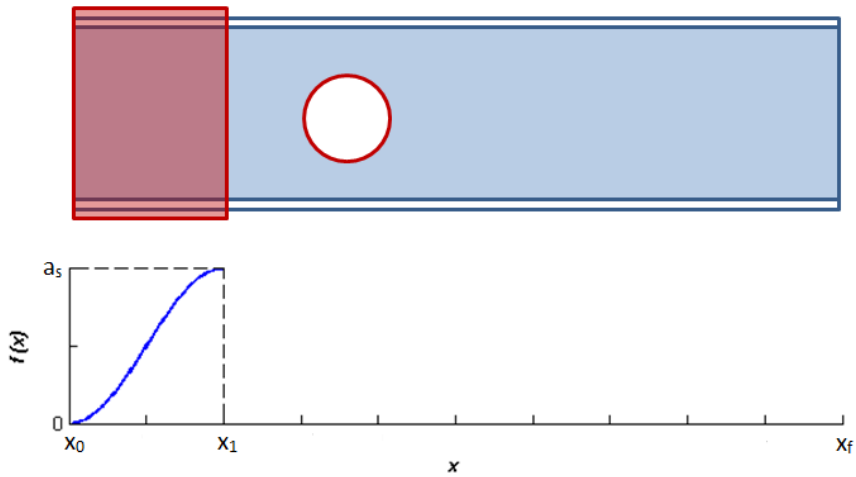


**Figure 4** Range of the flow conditioning region ($x_o$ to $x_1$) and shape function.

When a particle enters at the flow conditioner an additional term is taking into account in the calculation of the velocity in the explicit part of MPS algorithm. In the other words, instead of Eq. 9, which considers all the terms of the right hand side of the Navier Stokes equation except the pressure gradient term, Eq. 10 is adopted. Essentially, Eq. 10 introduces a numerical damping term and gradually adjust the velocity of the particles inside the flow

conditioning region in order to achieve the desired inlet velocity profile.

$$\left[\frac{D\vec{u}}{Dt}\right]_{exp} = \vartheta\nabla^2\vec{u} + \frac{\vec{f}}{\rho} + \vec{g} \tag{9}$$

$$\left[\frac{D\vec{u}}{Dt}\right]_{exp} = +\vartheta\nabla^2\vec{u} + \frac{\vec{f}}{\rho} + \vec{g} + \frac{\partial\vec{u}_{flux}}{\partial t} \tag{10}$$

In this first implementation of the technique, the velocity correction proposed is based on difference $\epsilon(u_x)$ and a shape function *f(x)*, where, *x* and $u_x$ are the *x*-axis position and *x*-component of velocity of each particle inside the flow conditioning region at the previous time step, respectively. Also, it is assumed that the desired upstream velocity profile for this study is a uniform profile of velocity *U*.

In the other hand, for the transverse component of the velocity are entirely suppressed at the beginning section of the flow conditioning region. This means when a particle with non null transverse component of velocity pass through $x_0$, the transverse component of its velocity is set to zero.

In this way, the numerical damping term adopted in the present study is:

$$\frac{\partial u_{x,flux}}{\partial t} = f(x)\epsilon(v_x) \tag{11}$$

The velocity difference is given by Eq. 11:

$$\epsilon(u_x) = U - u_x \tag{12}$$

The shape function *f(x)* modulates the intensity of the acceleration as a function the position on *x*-axis of the particle. The purpose of the shape function is induce a smooth and gradually velocity correction without discontinuity of computational domain, and to minimize the influence of the flow conditioning process on the flow upstream the conditioning region. The shape function used in this work is given by Eq. 12.

$$f(x) = a_0\frac{\sin\left(\pi\frac{x - x_0}{x_1 - x_0} - \frac{\pi}{2}\right) + 1}{2} \tag{13}$$

Where $a_0$ is an input parameter of acceleration intensity, $x_0$ and $x_1$ are the limits of the flow conditioning region.

The lower part of Figure 4 shows the curve of the shape function in relation of the computational domain. The sinusoidal shape provides a smooth transition near the start and ending sections of the flow conditioning region because its gradient is null in $x_0$ and $x_1$.

### 3.3 Simulation warming up

In the present work all the particles in the domain start from rest. In order to move the flow around an arbitrary shaped body, an acceleration field in the main stream direction is applied at the entire computational domain, as shown in the Figure 5.

In this warming up process, only the periodic boundary condition functions. The duration of the transient time interval is an input parameter of the simulation. To avoid that the transient interval last longer than the necessary, the duration of transient interval is estimated based on 1.5 times the necessary time to a particle in rest acquires velocity *U*. Also a

constraint limiting the velocity of the particles in the flow direction to $U$ is applied.

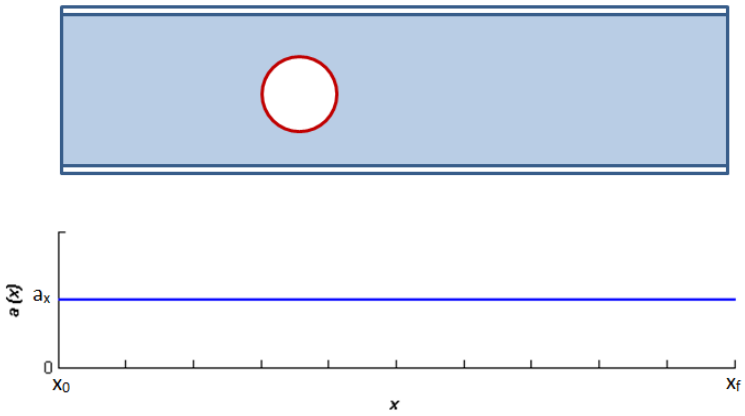


**Figure 5** Transient step acceleration field

## 4 WAKE AROUND A CIRCULAR CYLINDER

The potential of the particle method in simulating the flow around arbitrary shaped bodies includes a wide range of applications related to fluid solid interactions with complex geometry and multi-bodies. In this work, the basic case of flow around a fixed circular cylinder is considered. The dimensions of the model used in the simulations are presented at Figure 6. The red area indicates the flow conditioning region.

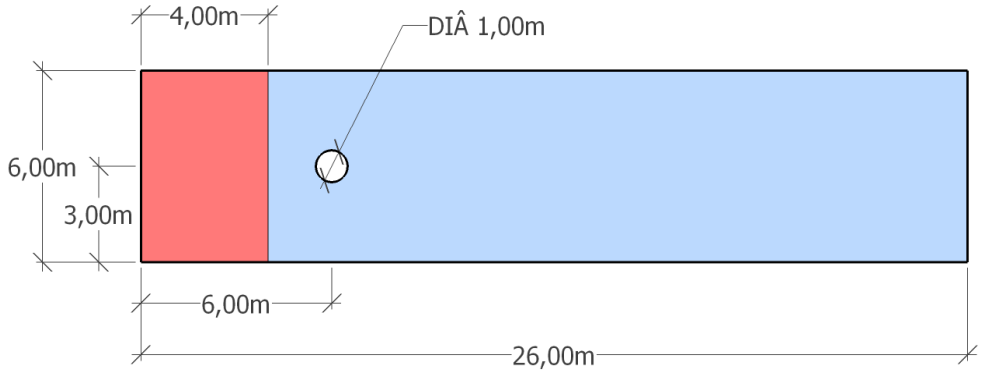


**Figure 6** Model dimension

### 4.1 Convergence analysis

The first step of the analysis comprises convergence study. Table 1 shows the three resolutions used in this section.

**Table 1 – Model resolutions**

| Particle distance [m] | D/dp | Number of particles | Simulation time |
|---|---|---|---|
| 0.1 | 10 | 7,074 | 5 min |
| 0.05 | 20 | 26,485 | 20 min |
| 0.025 | 40 | 102,331 | 7 hrs. |

First, a quantitative comparison between the snapshots of the simulations is given in Figure 7. In the top of Figure 7 is the field for *D/dp* = 10, where *D* is the diameter of the cylinder, and *dp* is the initial distance between the particles. In the middle of Figure 9 is the result for *D/dp*=20 and in the bottom for *D/Dp* = 40. Is observed that the result of the most coarse resolution significantly differs from the two another higher resolution ones, even the geometry of the cylinder is not well defined. But the two another resolution do not show such difference related to the velocity field of the flow, despite the geometry of the circular cylinder is not as prettily modeled.

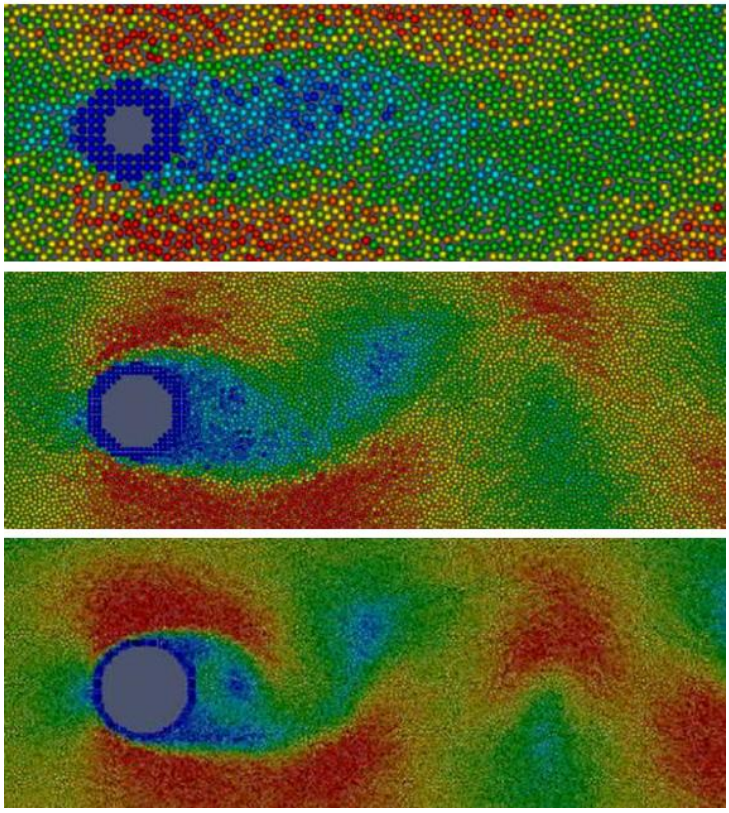

**Figure 7** Velocity magnitude field of Re = 1000 simulation – from top to bottom *D/dp* = {10, 20, 40}

The quantitative evaluation of convergence analysis is presented at Table 2, with the comparison of the pressure registered at the base point. The pressure in the base point oscillates due to the nature of vortex generation phenomenon.

**Table 2 – Convergence analysis – Pressure at base point**

| Particle distance [m] | D/dp | Mean pressure [Pa] | Standard deviation of pressure [Pa] | Standard deviation of pressure [%] |
|---|---|---|---|---|
| 0.1 | 10 | $1.77 \times 10^4$ | $5.66 \times 10^3$ | 31 |
| 0.05 | 20 | $1.81 \times 10^4$ | $3.48 \times 10^3$ | 19 |
| 0.025 | 40 | $1.72 \times 10^4$ | $3.12 \times 10^3$ | 16 |

Based on results presented at Table 2, all the resolutions show close results for the mean pressure, with the discrepancy from one to another less than 5 percent. On the other hand, the standard deviation of the pressure is much higher for the coarse resolution in relation to the other two resolutions, which show relatively close results. Therefore, an increasing in the resolution, from the $D/dp$ = 20 to $D/dp$ = 40 do not changed significantly neither the mean neither the standard deviation of the pressure. Thus the following simulations are based in models with $D/dp$ = 20.

Concluding the convergence analysis, in Table 3 are presented the numerical parameters used in the following simulations. The time step is estimated based on Courant number of 0.2, which results in the necessity of a time step above 0.001 seconds, considering the maximum velocity around 5 m/s for a flow with uniform velocity profile of $U$ = 3 m/s.

**Table 3 – Numerical parameter of the simulation**

| Particle distance [m] | D/dp | Time step [Pa] | Pressure smooth coefficient |
|---|---|---|---|
| 0.025 | 40 | 0.0005 | 0.075 |

## 4.2 Results

The present analysis of flow around a fixed cylinder is carried out by the considering 9 different Reynolds number flows, in a range from 50 to 100,000. The fluid density is 1,000 kg/m³. The inlet velocity profile is uniform with $U$ = 3 m/s. The Reynolds number is changed by modifying the fluid viscosity. The Table 4 presents the kinematic viscosity and the corresponding Reynolds number of the simulations performed in this study.

**Table 4 – Reynolds number of simulations**

| **Kinematic viscosity [m²/s]** | 0.06 | 0.03 | $6x10^{-3}$ | $3x10^{-3}$ | $6x10^{-4}$ | $3x10^{-4}$ | $6x10^{-5}$ | $3x10^{-5}$ |
|---|---|---|---|---|---|---|---|---|
| **Reynold number** | 50 | 100 | 500 | 1,000 | 5,000 | 10,000 | 50,000 | 100,000 |

The drift force time series, for a 5,000 Reynolds simulation, is presented in Figure 8. The blue curve shows the filtered data, i.e., after suppressing the characteristic spurious oscillations that are characteristics of the method. The amplitude of the filtered data is around 5,000 N/m and the amplitude of the unfiltered data. From the graph, the periodic nature of the vortex sheet generation process, which results in a oscillatory drift force over the cylinder, can be observed.

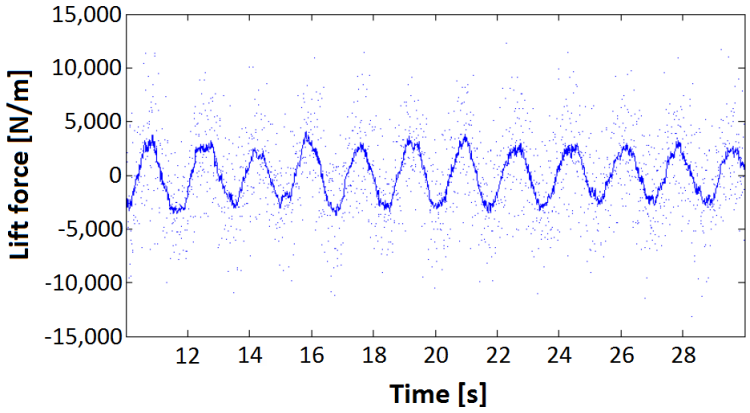


**Figure 8** Lift force over the cylinder for Re = 5000 – filtered (line) unfiltered (points)

The relation between the Strouhal number and the Reynolds number is a typical result of the flow around cylinders present in literature. The Strouhal number is a dimensionless number which describer oscillating flow mechanisms and is based on the frequency of vortex generation on the vortex sheet. The frequency of the generation of vortex is obtained by the lift force time series such as presented in Figure 8. In Figure 9 gives the diagram of Strouhal number as a function of Reynolds number for the flow around a fixed circular cylinder. Figure 9-a is the diagram based on experimental results extracted from [4], and Figure 9-b shows the results obtained from the MPS simulations. The comparison between the two diagrams show that the values of Strouhal numbers are almost constant along the range of Reynolds number considered in the present study, and they are around 0.2. Also, the experimental data and the numerical result show relatively close results.

(a) (b)

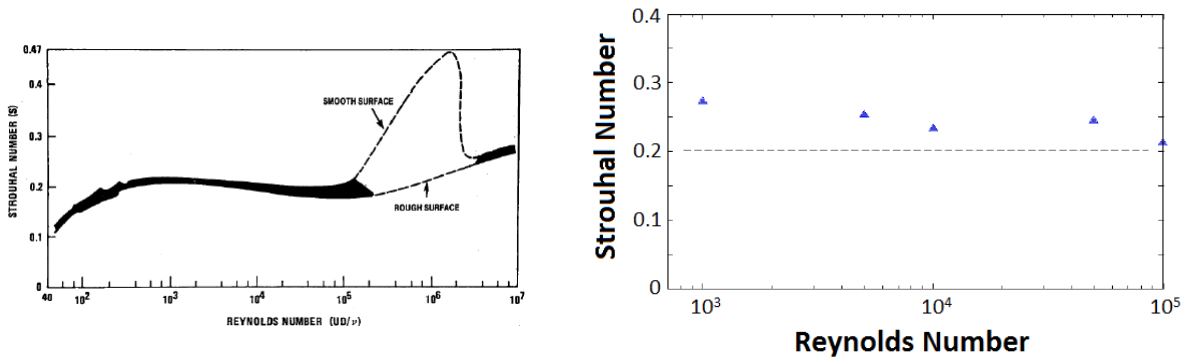


**Figure 9** Reynolds Number x Strouhal Number diagram –Experimental results from Blevins [4] (a) numerical results obtained by MPS (b)

Figure 10 shows the streamlines, with the formation of a symmetrical pair of vortex, expected in the literature for the Reynolds number range from 5 to 40 and simulated for the Reynolds number of 50. This result shows that the particle method simulation shows the same behavior as expected by the results in literature for similar Reynolds number.

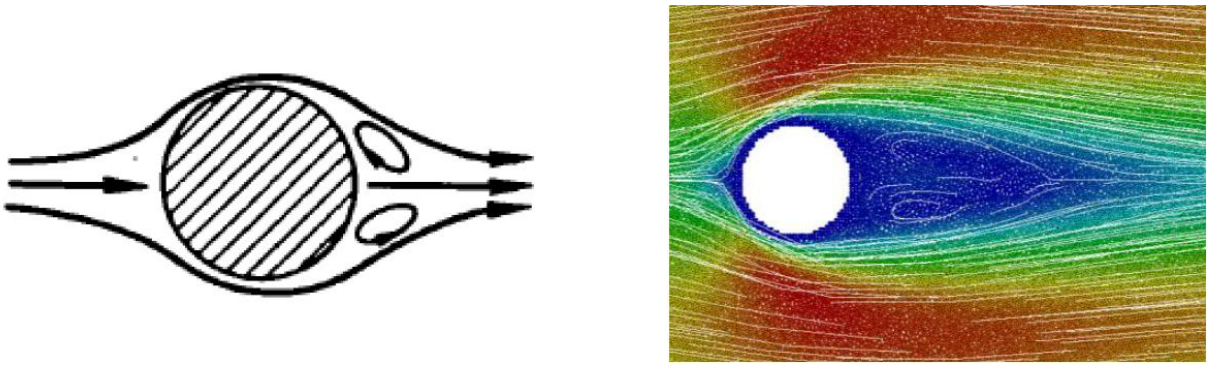

**Figure 10** Wave of a pair of vortex – Streamlines from [4] (5<Re<40)(left) and streamlines obtained by MPS (Re = 50)(right)

## 6 CONCLUDING REMARKS AND NEXT STEPS

In the present work a recirculation boundary condition is proposed in order to investigate the complex interaction of flow and arbitrary shaped bodies. The development of the recirculation boundary condition succeeded on its purposes of simplify the modeling of the boundary conditions in the inflow and ouflow boundaries. The recirculation boundary condition operates such as a shortened recirculation tunnel or canal, and is composed by a periodic boundary condition and a flow conditioner. The periodic boundary condition re-inject on the upstream boundary the particles that reach the downstream boundary. In the other hand, the flow conditioner adjusts the flow upstream the body to an expect velocity profile, by eliminating the velocity perturbations and accelerating the flow downstream of the body.

To verify the effectiveness of the recirculation technique, a simple case of flow around a circular cylinder was studied. The comparison between the results present in literature and the numerical results obtained by applying the proposed approach for the flow around a fixed circular cylinder shows relatively nice agreements.

The next steps of this research topic are related to the investigation of the mechanism of the flux controller, related to an optimization based on the analysis of the shape function and the relation between the error function and the numerical damping term. The objective of this optimization is obtain an optimal shape function and parameter in order to achieve a minimal flow conditioning region.

## ACKNOWLEDGEMENTS

The authors thank PETROBRAS for the financial support during the development of the numerical simulator in Numerical Offshore Tank (TPN-USP). The author also thanks PRH-19 of National Petroleum Agency of Brazil (ANP) for the scholarship.

## REFERENCES

[1] S. Koshizuka, H. Tamako and Y. Oka, "A particle method for incompressible viscou flow with fluid fragmentation," *International Journal of Computational Fluid Dynamics,* vol. 4, pp. 29-46, 1995.

[2] M. M. Tsukamoto, L.-Y. Cheng and K. Nishimoto, "Analytical and numerical study of the effects of an elastically-linked body on sloshing," *Computer & Fluids,* vol. 49, pp. pp. 1-21, 2011.

[3] L.-Y. Cheng, D. V. Gomes, A. M. Yoshino and K. Nishimoto, "Numerical simulation of oil leakage, water flooding and damaged stability of oil carrier based on Moving Particles Semi-implicit Method," in *The proceedings of the 2nd Intenational Conference on Particle-Based Methods (PARTICLES 2011)*, Barcelona, Spain, 2011.

[4] R. D. Blevins, Flow-Induced Vibration, Malabar, Florida: Krieger Publishing Company, 1990.